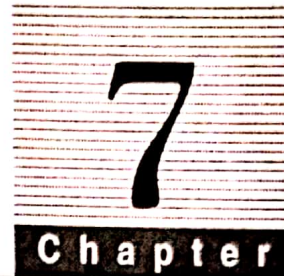


Semiconductor Materials Processing



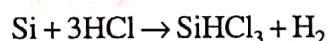
7.1 Crystal Growing

Silicon and germanium are two of the most widely used semiconductor materials. Of these two, silicon has been dominant since it was first used in early 1950s. The widespread use of Si is based on various favorable factors attached with the material.

- ✓ It is most abundant element after oxygen in the earth. Around 28% of earth is composed of silicon.
- ✓ The raw material from which pure silicon is extracted is found everywhere in the nature. So, it is very cheap.
- ✓ The natural oxide of silicon SiO_2 is an excellent insulating medium.
- ✓ It has good heat conductivity, which is also favorable for many applications.
- ✓ The energy band gap is enough large to be used in various applications. But not so large to cancel out their usefulness.
- ✓ It is non-toxic. So, no special care is needed when using Si for industrial and commercial applications.

Pure silicon is required for various applications. In nature, there is no pure silicon. It can be found in compound form only. So there are certain procedures to obtain pure silicon as explained below.

- SiO_2 is heated to high temperature in a reducing environment to obtain approximately 98% pure silicon powder.
- The silicon powder is then reacted with HCl gas to form trichlorosilane gas.



which is then distilled and reduced with hydrogen to form polycrystalline silicon (reverse of above process).

- The polycrystalline silicon is then melted and cast into ingots, from which the single crystal is obtained.

There are basically two methods of obtaining pure silicon crystals:

- (i) Floating zone refining and crystal growth
- (ii) Czochralski growth.

7.1.1 Floating Zone Method of Crystal Growth

This method, in addition to, being capable of producing single crystals and also removing the extra impurities contained in the semiconductor material. The impurities can be removed very easily as they prefer to go to the liquid phase.

This type of crystal growing material is rarely used because of the high temperature requirement of silicon, there is always possibility of silicon crystals adhering to their crucible wall which causes deviation from the perfect lattice structure required for the silicon crystal.

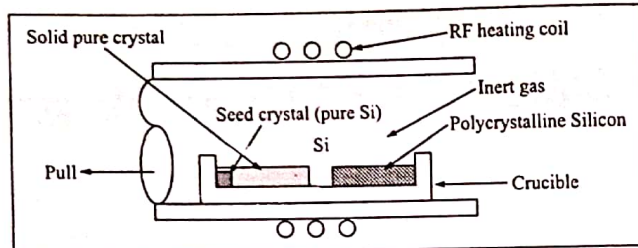


Fig. 7.1 Floating zone method of crystal growing

The RF (Radio-frequency) heating coils heats the crucible in which the polycrystalline silicon is placed. As the Si is heated, it melts at high temperature and by solidification by slowly pulling it to the left where there is seed crystal; single pure crystal for IC fabrication is obtained. The inert gas is used to suppress evaporation and prevent oxidation.

7.1.2 Czochralski Growth

Large, single, Si crystals are grown by Czochralski method, which involves growing a single crystal ingot from the melt using solidification on a seed crystal. Molten Si is held in quartz crucible in a graphite susceptor, which is heated by a RF heating coil. The seed crystal is lowered to touch the melt and then

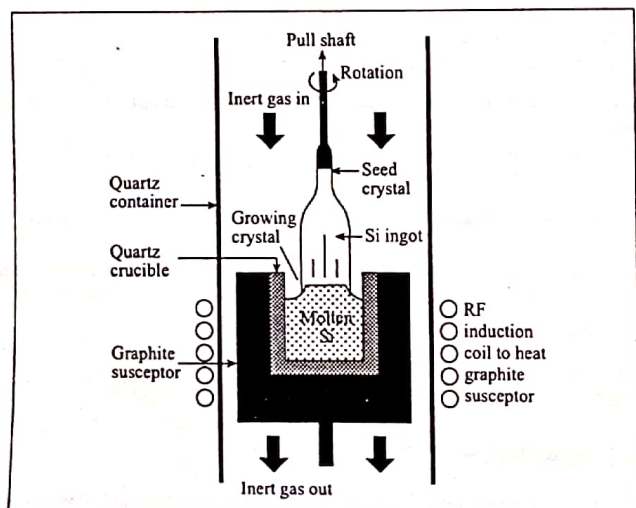


Fig. 7.2 Single crystal growth by Czochralski method

slowly pulled out of the melt. In solidification pure crystal grows. The seed is rotated during pulling stage, to obtain a cylindrical ingot. To suppress evaporation from the melt and prevent oxidation inert gas is used.

Initially, as the crystal is withdrawn, its cross-sectional area increases; it then reaches a constant value determined by the temperature gradients, heat losses, and rate of pull. As the melt solidifies on crystal, heat of fusion is released and must be conducted away, otherwise it will raise the temperature of the crystal and re-melt it.

The above mentioned processes will result in single crystal rods being formed. These rods are sliced by a diamond band saw, etched and polished to obtain wafers that are 0.3 to 0.4 mm thick. These wafers are the basic building blocks for device fabrication.

7.2 Diffusion System

7.2.1 Diffusion

This is one of the primary methods of introducing impurities such as boron, phosphorous, antimony into silicon to control the majority-carrier type and sheet resistivity of layers formed in the wafer. Diffusion process begins with the deposition of a high concentration of the desired impurity on the silicon surface through windows etched in the protective barrier layer. At high temperatures (900–1200°C), the impurity atoms move from the surface into the silicon crystal by substitutional or interstitial diffusion mechanisms. In substitutional diffusion, the impurity atom hops from one crystal lattice site to another. The impurity atom substitutes for a silicon atom in the lattice. There must be vacancies in the lattice for this process to go on, and the vacancies generally exist in the lattice. At high temperatures, the silicon atoms are displaced from their usual positions to interstitial space between lattices, and vacancies are created. The substitutional diffusion process in which impurities are introduced and silicon atoms are displaced into interstitial sites is called interstitial diffusion.

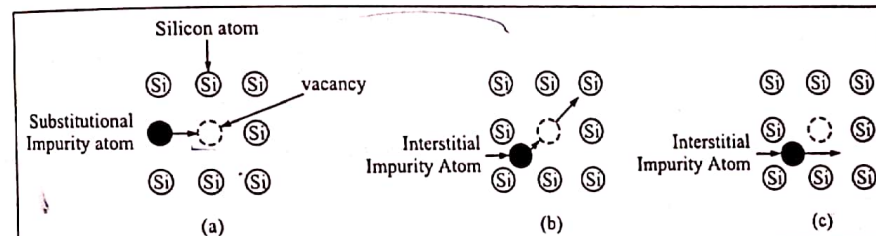


Fig. 7.3 Two dimensional Si lattice. Substitutional diffusion (a); Interstitial, in which impurity atom replaces the Si atom (b); Interstitial diffusion in which impurity atom does not replace Si atom in crystal lattice (c).

The mathematical expression of diffusion process in 1-dimension can be derived using Fick's laws of diffusion. Fick's first law of diffusion states that the particle flow per unit area (particle flux), J , is directly proportional to concentration gradient of the particle.

$$J = -D \frac{\partial N}{\partial x} \quad (7.1)$$

where N is the particle concentration and D is the diffusion coefficient. The $-ve$ sign indicates that particles move from region of high concentration to low concentration.

The continuity equation for particle flux is

$$\frac{\partial N}{\partial t} = -\frac{\partial J}{\partial x} \quad (7.2)$$

Combining equations (7.1) and (7.2) gives Fick's 2nd law of diffusion:

$$\frac{\partial N}{\partial t} = D \frac{\partial^2 N}{\partial x^2} \quad (7.3)$$

Two specific boundary conditions, namely, constant source diffusion and limited-source diffusion are important in modeling the diffusion.

7.2.1.1 Constant-source diffusion

During constant source diffusion, the impurity concentration is held constant at the surface of wafer. As time progresses, the diffusion front proceeds further and further into the wafer with the surface concentration remaining constant. The number of impurity atoms per unit area in Si called dose, Q , increases with time, and an external impurity source must supply a continual flow of impurity atoms to the surface of wafer.

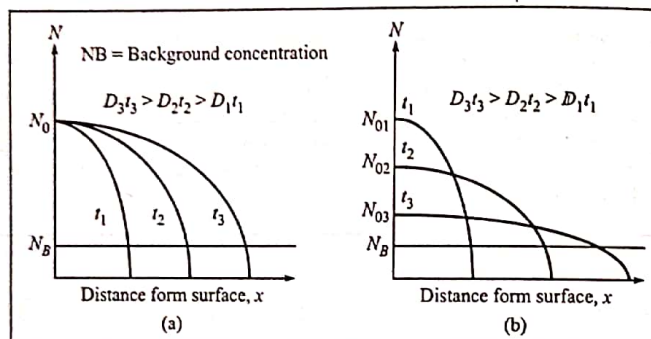


Fig. 7.4 A constant source diffusion (a); limited source diffusion (b).

7.2.1.2 Limited source diffusion

In this process the dose remains constant throughout the diffusion process. As the diffusion front moves into the wafer, the surface concentration must decrease so that the area under the curve can remain constant with time.

A short constant source diffusion is often followed by a limited source diffusion, resulting in a two step diffusion process. The constant course diffusion is used to establish a known dose in a shallow layer on the surface of the silicon and is called the preposition step. The second diffusion called the drive-in step is used to move the diffusion front to the desired depth.

7.2.1.3 Junction formation by vertical diffusion

The goal of most diffusions is to form pn junctions by converting p-type material to n-type and vice versa. The point at which the diffused impurity profile intersects the back-ground concentration N_B is called metallurgical junction depth x_j . The net impurity concentration at x_j is zero.

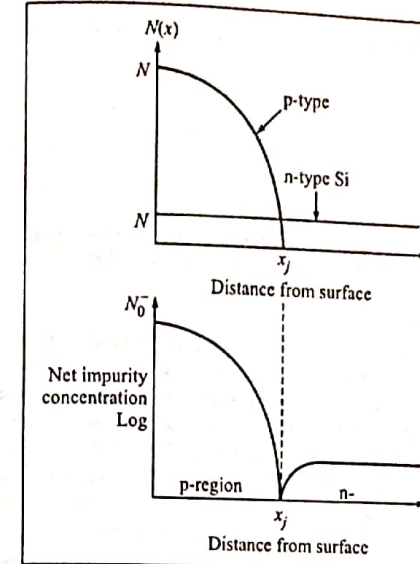


Fig. 7.5 Formation of pn junction. P type diffusion into n type wafer (a); Net impurity concentration in the wafer (b).

7.2.1.4 Lateral diffusion

During diffusion, impurities not only diffuse vertically but also move laterally under the edge of any diffusion barrier. Lateral diffusion is an important effect coupling device and process design and was an important factor driving the development of self-aligned polysilicon-gate MOS processes.

7.2.1.5 Sheet resistance

In diffused layers, resistivity is a strong function of depth. For circuit and device design, it is more convenient to express sheet resistance, which is given by equation (7.4).

$$R = \rho \frac{L}{A} \quad (7.4)$$

where ρ = resistivity of the material,

L = length

A = cross-sectional area of the material

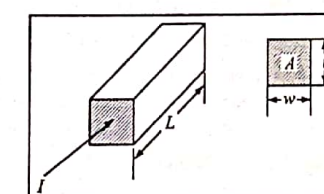


Fig. 7.6 Resistance block of material having uniform resistivity.

Using w as width and t as thickness of the block, cross-sectional area $A = wt$ and the resistance of the block can be written as

$$R = \rho \frac{L}{A} = \rho \frac{L}{wt} = \frac{\rho L}{t w}$$

$$R = R_s \frac{L}{w} \quad (7.5)$$

where R_s is called sheet resistance of layer of material. If sheet resistance is given, a circuit designer needs to specify only the length and width of the resistor to define its value.

7.2.1.6 Diffusion systems

The open-furnace-tube system using solid, liquid, or gaseous sources is the most common diffusion technology used in IC production. Wafers are placed in a quartz boat and positioned in the center zone of the furnace, where the wafers are heated to high temperatures. Impurities are transported to silicon surface, where they diffuse into the wafer. In solid source system, carrier gases N_2 or O_2 flow at a controlled rate over a source boat placed in the furnace tube as shown in fig. 7.7.a. The carrier gas picks up the vapour from the source and transports it down the tube, where the dopant species is deposited on the surface of wafer. The temperature of the source is controlled to maintain the desired vapour pressure.

In liquid source system shown in fig. 7.7.b, a carrier gas passes through a bubbler where it picks up the vapour of the liquid source. The gas carries the vapour into the furnace tube where it reacts with the surface of the silicon wafer.

In gas source system, the dopants are directly supplied to the furnace tube in the gaseous state. The common gas source are extremely toxic, and additional input purging and trapping systems are required to ensure that all the source gas is removed from the system before wafer entry or removal.

B , P , As and Sb are the most common dopants used diffusion. Of these, B is the most popular p-type dopant due to its high solubility in silicon and high surface concentration of 4×10^{20} per cm^3 . Also, the elemental boron is inert up to temperatures exceeding the melting point of silicon. A surface reaction with boron trioxide is used to introduce boron into the silicon surface: $2B_2O_3 + 3Si \leftrightarrow 4B + 3SiO_2$ (7.6)

Common solid source of boron are trimethylborate(TMB) and boron nitrate wafers. TMB vapour reacts in furnace tube with oxygen to form boron trioxide:



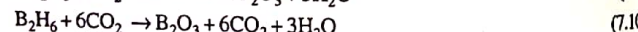
The most common liquid source of boron is boron tribromide. The reaction is:



The primary gaseous source of boron is diborane. The reaction is:



or



Phosphorous which is common n-type dopant used in diffusion has higher solubility in silicon than boron and has a surface concentration in the range of 10^{21} per cm^3 during high temperature diffusion. P is introduced into Si through the reaction of phosphorous pentoxide at the wafer surface.

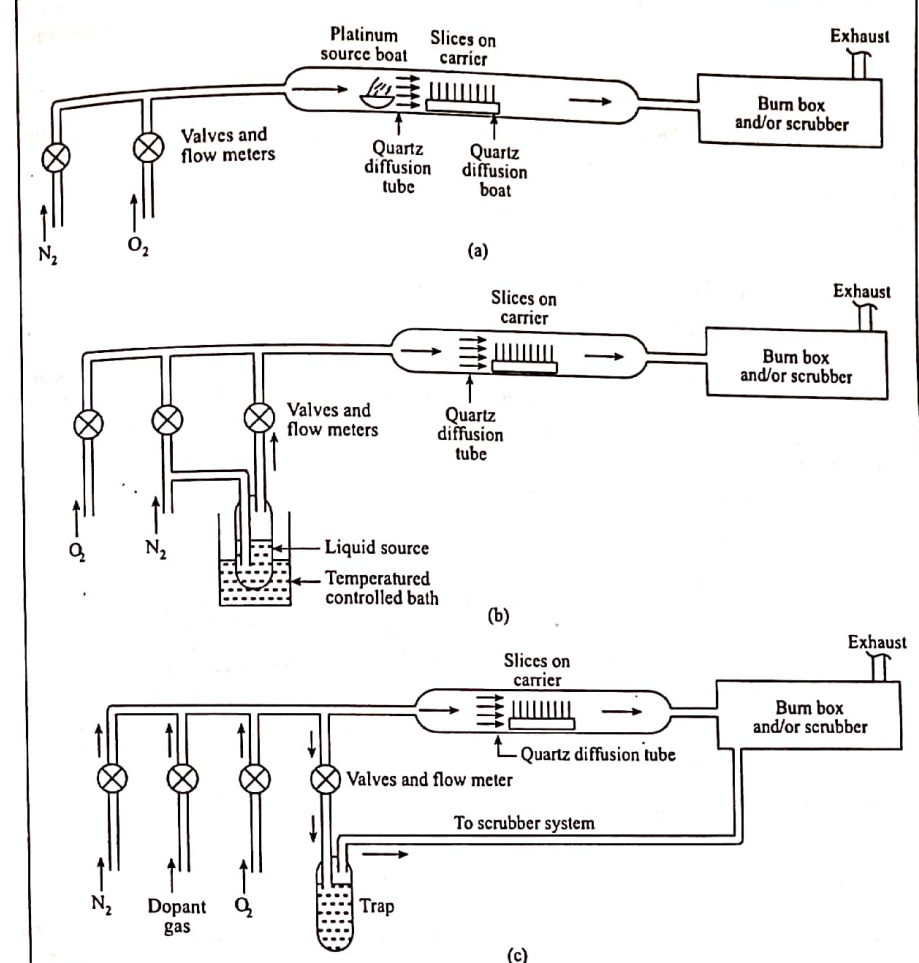
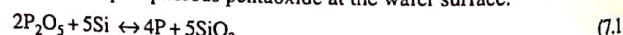


Fig. 7.7 Open furnace tube diffusion system. Solid impurity source (a), liquid impurity source (b) and gaseous impurity source (c)

Solid wafers of phosphorous pentoxide can be used as source for phosphorous. The reaction to obtain P_2O_5 by using phosphorous oxychloride $POCl_3$ and oxygen is:



Phosphine is used as gaseous source for phosphorous.



Arsenic has the highest solubility among the dopants in silicon, with surface concentration reaching 2×10^{21} per cm^2 . The oxide vapours are carried into the furnace tube from a solid diffusion source by a N gas carrier. Evaporation of As limits the surface concentration to below 3×10^{19} per cm^2 . Arsenic gas is extremely toxic. The surface reaction involving arsenic trioxide is:



Antimony diffusion is done by using antimony trioxide as solid source which is placed in a two-zone furnace in which is maintained at a temperature of 600 to 650°C. The reaction to introduce antimony into the silicon is:



7.3 Ion Implantation Process

7.3.1 Ion Implantation

Ion Implantation process has many advantages over diffusion for the production of impurity atoms into the silicon wafer, so is the most widely used technology in modern IC fabrication. An ion implanter is a high-voltage particle accelerator producing a high-velocity beam of impurity ions, which can penetrate the surface of Si wafers.

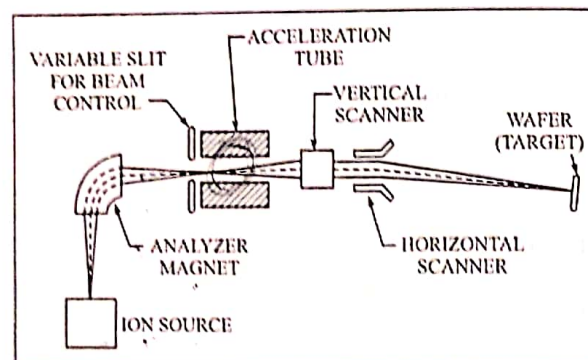


Fig. 7.8 Typical Ion Implanter

The ion source, which operates at high voltage (25kV), is meant for producing plasma containing desired impurity, but it produces undesired impurities as well. An analyzer magnet bends the ion beam through a right angle to select the desired impurity ion, which then passes through an aperture slit into the main accelerator column. The main function of accelerator column is to add energy of up to 175 keV to the beam and accelerate the ions to their final velocity. Scanning system consists of x- and y-axis deflection plates to scan the beam across the wafer to give a uniform implantation and to build up the desired dose. The beam is bent slightly to prevent neutral particles hitting the target. The target chamber has silicon wafers, which will be targeted by the impurity ions.

A charged particle with velocity v in magnetic field B will experience a force F given by

$$F = q(vxB) \quad (7.16)$$

The force will tend to move the particle in a circle, and the centrifugal force will balance F . But, $qvB = mv^2/2$ and $mv^2/2 = qV$. So the magnitude of magnetic field B can be adjusted to select an ion species with a given mass:

$$|B| = \sqrt{(2mV/qr^2)} \quad (7.17)$$

where V – acceleration voltage,
 r – velocity of particle.

The ion source operates at constant potential, so voltage is known. So the ion species is selected by changing dc current supplying the magnetic analyzer. The target chamber is maintained at relatively low temperatures during the implantation, which prevents undesired spreading of impurities by diffusion – very important in VLSI fabrication. Also, by ion implantation wide range of impurities can be implanted compared to that of diffusion. The main drawback is the cost of the ion implanter.

Ion implantation usually follows a Gaussian distribution as given by:

$$N(x) = N_p \exp \left[-\frac{(x - R_p)^2}{2\Delta R_p^2} \right] \quad (7.18)$$

where $N(x)$ is the impurity concentration,
 N_p is the peak concentration,
 R_p – the projected range
 ΔR_p – standard deviation called straggle

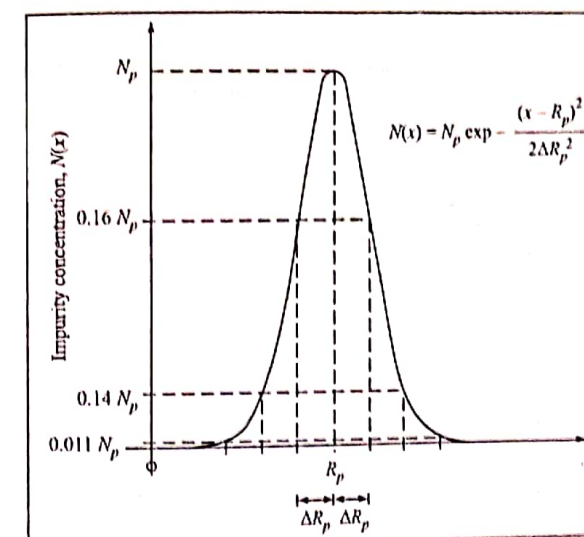


Fig. 7.9 Gaussian distribution resulting from ion implantation. The impurity is shown implanted completely below the wafer surface ($x = 0$).

The ion implantation is often used to form shallow pn junctions for various device applications where the junction depth can be found by equating the implanted distribution function to the background concentration N_B as:

$$N_P \exp \left[-\frac{(x_j - R_p)^2}{2\Delta R_p^2} \right] = N_B$$

or

$$x_j = R_p \pm \Delta R_p \sqrt{2 \ln(N_P/N_B)} \quad (7.19)$$

7.3.2 Lattice Damage and Annealing

During the implantation process, an ion impact can knock atoms out of Si lattice, damaging the implanted region in the crystal. For higher doses, the implanted layer becomes amorphous. With heavier impurities lower doses will be required to create an amorphous layer.

Implantation damage can be removed by annealing. After the implantation, the wafer is heated to a temperature $\sim 900^\circ\text{C}$ for approximately 30 minutes. At this temperature, Si atoms can move back into lattice sites, and impurity atoms can enter substitutional sites. After annealing cycle, nearly all of the implanted dose becomes electrically active, except for impurity concentration exceeding 10^{19} cm^{-3} . Truly amorphous layers can be annealed at lower temperatures through solid-phase epitaxy.

7.3.3 Chemical Vapour Deposition

Chemical vapour deposition (CVD) forms thin films on the surface of a substrate by thermal decomposition and/or reaction of gaseous compound. The desired material is deposited directly from the gas phase onto the surface of substrate. Polysilicon, silicon dioxide and silicon nitride are deposited using CVD technique. CVD can be performed at pressures for which the mean free path for gas molecules is quite small.

Si is deposited in low pressure chemical vapour deposition (LPCVD) by using thermal decomposition of silane.



Low-pressure systems use either 100% or 25-30% silane diluted with nitrogen.

Silicon dioxide can be deposited by using silane and oxygen:



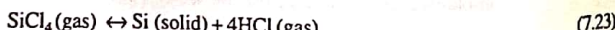
Phosphorous pentoxide can be deposited by using phosphine and oxygen as:



7.3.4 Epitaxial Growth

Epitaxial growth comes from Greek word "epitaxy" meaning "arranged upon". The growth of a single crystalline layer from the vapour phase is called vapour-phase epitaxy. Liquid-phase epitaxy and molecular-beam epitaxy are also widely used in GaAs technology.

Silicon tetrachloride (SiCl_4), Silane (SiH_4), dichlorosilane (SiH_2Cl_2) and trichlorosilane (SiHCl_3) are most commonly used for silicon vapour phase epitaxy.



The reaction takes place at approximately 1200°C and is reversible.

Epitaxial growth can also be achieved by pyrolytic decomposition of silane:



The reaction is not reversible and takes place at low temperature.

In liquid-phase epitaxy, the substrate is brought into contact with a solution containing the material to be deposited in liquid form. The substrate acts as a seed for material crystallizing directly from the solute.

In liquid phase epitaxy, the substrate is brought into contact with a solution containing the material to be deposited in liquid form. The substrate acts as seed for material crystallizing directly from the solute.

In molecular beam epitaxy, the crystalline layer is formed by deposition from a thermal beam of atoms or molecules in ultrahigh vacuum conditions. Substrate temperature during this process ranges from 400-900°C.

7.4 Monolithic IC Fabrication: Planar Process

In the planar process, the fabrication of the IC is done plane by plane at one surface of the wafer so that the deepest doped region tends to be fabricated first. We will consider fabrication of two neighbouring integrated npn bipolar junction transistors. At first, heavily doped n^+ buried layers of all npn BJTs are fabricated. For this, a silicon wafer, in the form of thin p-type single Si-crystal, is oxidized in an oxidation furnace to form a thin layer of SiO_2 , which is excellent barrier against diffusion. The silicon dioxide layer adheres to the Si crystal without any cracks and pores and forms a continuous layer with an amorphous structure. SiO_2 can be easily etched to open windows to allow diffusion of dopants through selective areas. A process called lithography, which literally means writing on stone, provides a means for defining windows in the oxide. The surface of the oxidized wafer is coated with a thin photoresist emulsion. A positive photoresist, which becomes chemically soluble when exposed to UV light will be considered here. A black and white photomask is fabricated in which the white areas correspond to regions where diffusion windows are needed in SiO_2 . The wafer is illuminated by UV light, which causes photoresist regions under transparent areas of photomask become soluble by UV light. Then the photoresist is developed in a suitable chemical solution in which soluble regions are chemically washed away and only insoluble region remain. The photoresist mask that remains on the oxide is hardened to resist etchant to be used for oxide removal. Windows are then etched in oxide by using an etchant (HF acid). The process in which UV light is used to reproduce the diffusion window pattern is called photolithography. Once Si crystal surface has been accessed through the diffusion windows, donor dopants are diffused into crystal. The surface region where diffused donors exceed the bulk acceptor concentration becomes n -type by compensation doping. By suitable temperature and pressure, heavy n -type doping is done to form n^+ doping. The SiO_2 used in n^+ buried layers diffusion is removed by etching, and then a thin lightly doped epilayer is grown on the surface. The entire diffused and doped region occurs in the epilayer. Individual components must be isolated from each other by embedding each component in n -type island and p -type island. The whole crystal is reoxidized and using photolithography next set of window patterns are defined. Windows are then etched around each collector region (fig 7.10.i). Acceptor impurities are then diffused to the substrate to form p^+ regions around each collector (fig 7.10.j). The whole crystal is again reoxidized and the new oxide grows on the surface of the already present oxide as well as Si crystal (fig 7.10.k). Photolithography is used once again and diffusion windows are then etched (7.10.l). Boron gas is diffused through the windows to form a lightly p -type base (7.10.m). Once again using photolithography new windows are etched in the oxide where n^+ emitter region and n^+ ohmic contacts to the collector are to be formed (7.10.n). Donor dopants are then introduced to form n^+ emitter regions and n^+ contact regions of the collector (7.10.o). The bipolar fabricated at the end of step o need contacts and interconnections. For this the whole surface is

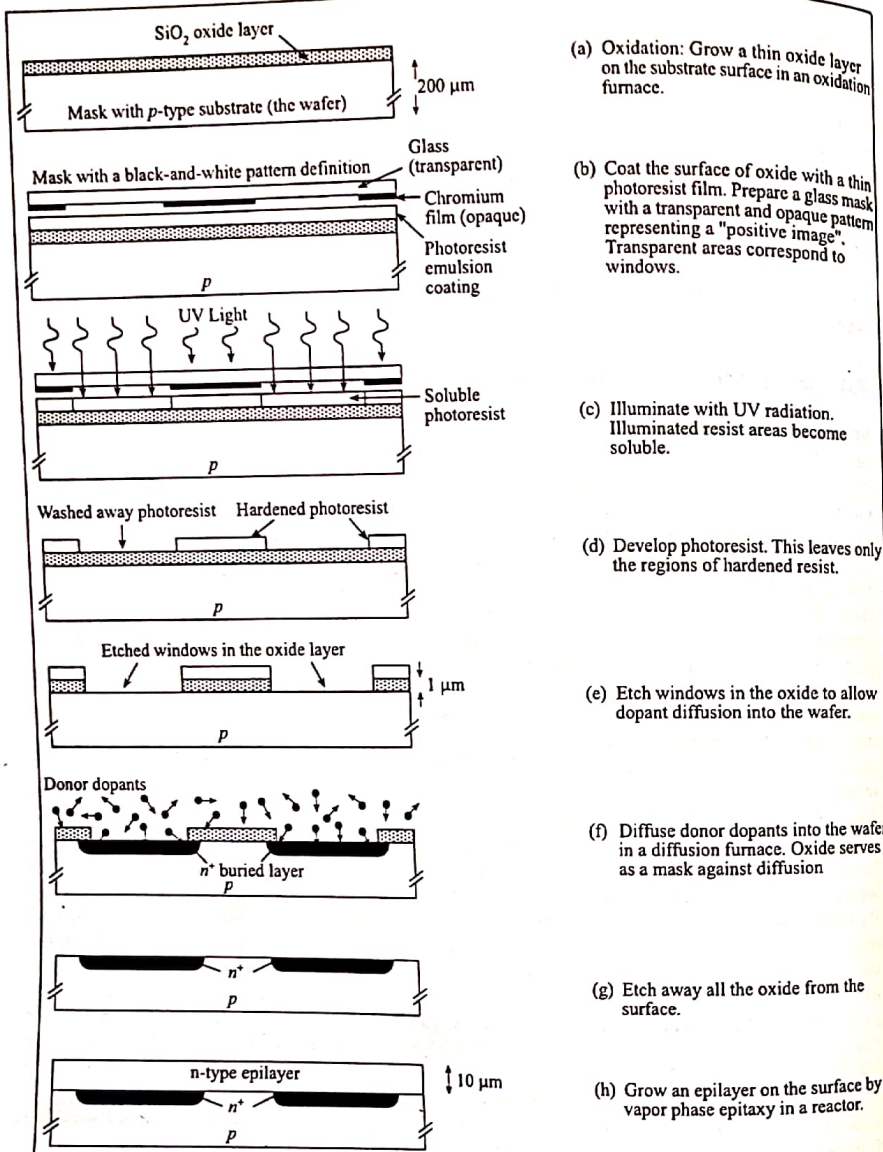


Fig. 7.10(a-h) Planar Process of IC fabrication

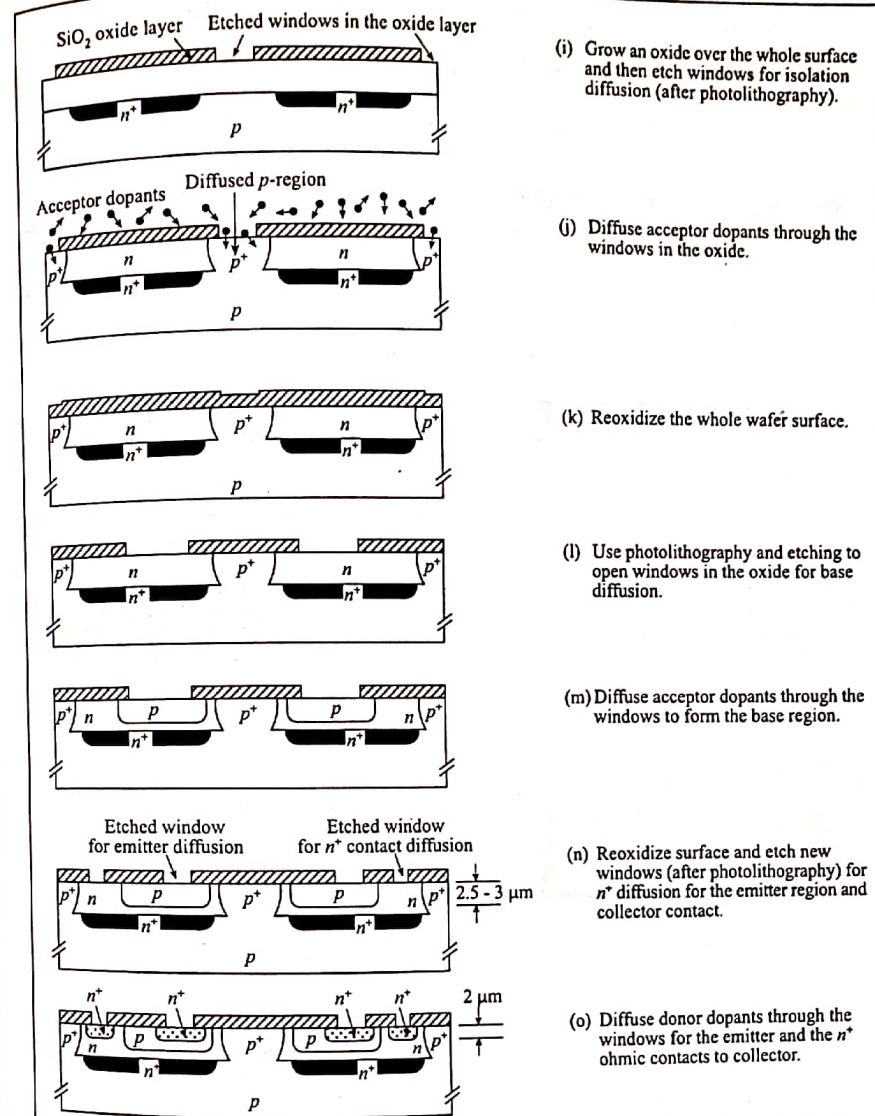


Fig. 7.10(i-o) Planar Process of IC fabrication

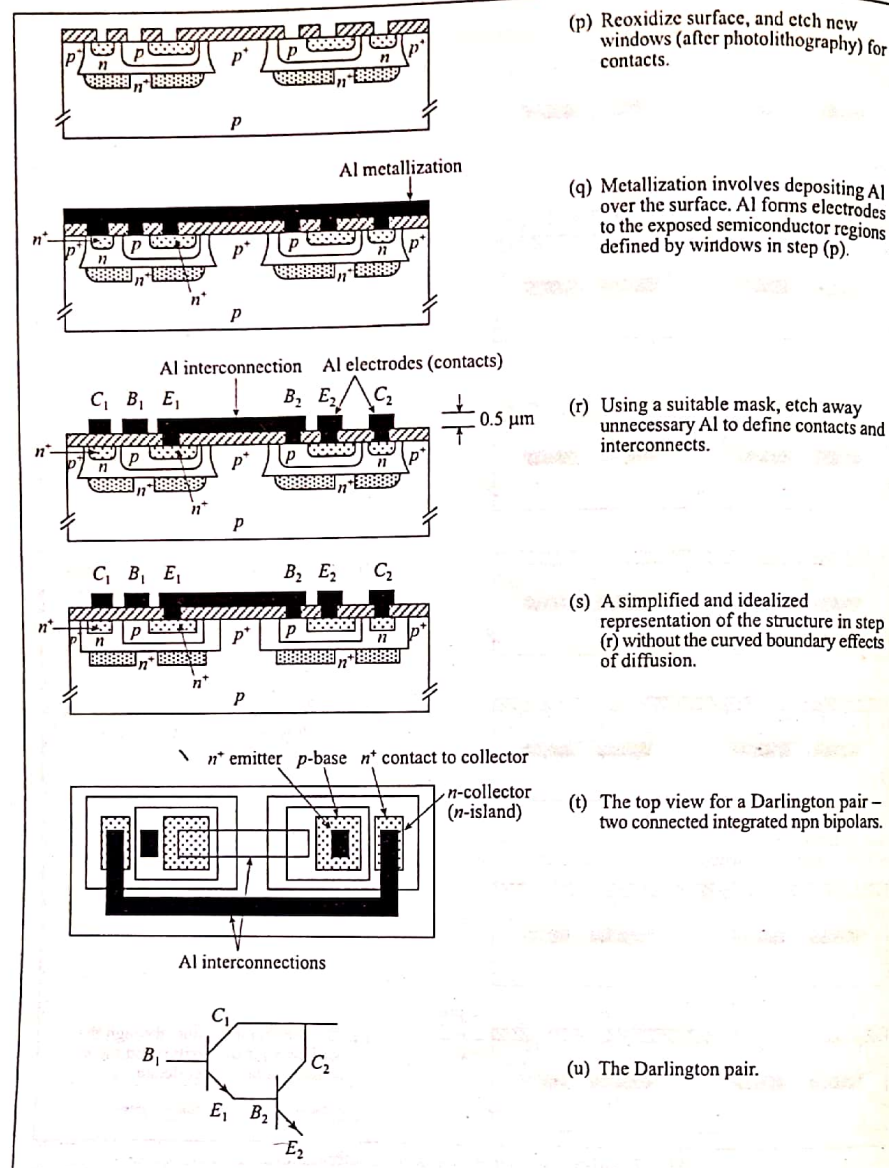


Fig. 7.10(p-u) Planar Process of IC fabrication

reoxydized and using photolithography, the oxide is masked by a photoresist pattern and windows are etched where contacts are needed (fig 7.10p). Aluminum is coated over the whole surface of the wafer (7.10q). The aluminum covering the whole surface area is etched selectively to remove all unwanted aluminum except where the metal is needed for interconnection (7.10r). After the formation of interconnection, each chip on the offer is electrically tested and those failing would be marked and discarded. After the testing, the wafer is diced, scribed with a diamond stylus, to individual IC chips. Each chip is mounted, bonded to leads, and encapsulated in a package that is suitable for application.

7.5 Metallization, Contacts

The requirement of low-resistivity materials leads one to consider the use of metals as interconnections. Aluminum is mostly used being cheaper and adheres to SiO_2 . Aluminum may contact semiconductor regions in different ways as shown in fig 7.11. Aluminum contact to p-type Si normally results in a good ohmic contact for doping levels exceeding 10^{16} cm^{-3} . But for lightly doped n-region, Schottky junction can be formed between metal and semiconductor.

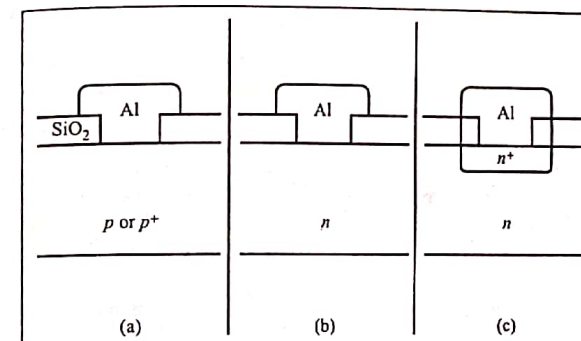


Fig. 7.11 Aluminum to p-type sc forms ohmic contact (a), aluminum to n-type forms Schottky junction (b) and Aluminum to n^+ region forms practical non-linear ohmic contact (c).

There is small resistance associated with an ohmic contact between two materials.

$$R_c = \frac{\rho_c}{A} \quad (7.25)$$

where ρ_c – specific contact resistivity, $\text{ohm}\cdot\text{m}^2$,
 A – area of the contact.

Aluminum contacts to silicides suffer from pitting and spiking problems. To circumvent these problems, an intermediate layer of metal is used to prevent silicon diffusion. In fig 7.11, titanium-tungsten (TiW) is used as a barrier metal over silicides in the contact regions of both bipolar and MOS technologies. The final contact consists of a sandwich of a silicide over the diffusion, followed by TiW diffusion barrier, and completed with aluminum copper interconnection metallization.

In most of the applications, a single layer of metal does not provide sufficient capability to fully interconnect complex VLSI chips. So, many processes use two or three levels of polysilicon as well as several levels of metallization in order to ensure wirability and provide adequate power distribution.

Superconductivity

Chapter 8

8.1 Introduction

The electrical resistance of metal and alloys decreases with the decrease of temperature. At lower temperature, the thermal vibrations of the atoms decrease. So due to decrease in randomness of free electrons, resistance decreases. When a specimen of material is cooled sufficiently low temperature in the liquid helium range, resistivity drops to zero. The phenomenon was first observed in 1911 by Dutch Physicist Kamerlingh Onnes who discovered that the electrical resistance of mercury drops to zero (see Fig 8.1.) at temperature of about 4K. He found that below this temperature, the resistance remained effectively zero. Electrical current flowed in the mercury in the absence of potential difference and without causing the heating associated with the electrical resistance in the conductors. Onnes declared that "no doubt was left of a new state of mercury in which its resistance has practically vanished. Mercury has passed into a new state which on account of its extra ordinary properties may be called the superconductive state".

When a superconductor is cooled below a certain temperature, there is not only an abrupt loss of electrical resistance as discovered by Onnes but there are also abrupt changes in many properties of the materials. All these changes take place at a same temperature which is known as critical temperature (T_c). Below the critical temperature, the material is **superconductive state** and above the critical temperature, the material is **normal state**. The temperature at which transition between the superconductive state and normal state occurs is in the absence of magnetic field independent of shape or size of the specimen. It is a characteristic of material.

Before 1986, the superconductivity was rather low temperature phenomenon and is a definite obstacle to its technological exploitation, since it means that a superconducting device has to be accompanied refrigeration equipment of some kind to keep the temperature sufficiently low. Even only 125K or just one decade above the temperature, i.e. critical temperature has obtained in the compound $Tl_2Ba_2Ca_2Cu_3O_{16}$ (TBCCO) in the IBM institute. Most of the scientists of the world are working to obtain at room temperature. Experimentally and theoretically they have concluded that:

- (I) No ferromagnetic or anti-ferromagnetic materials are superconductor. There is diamagnetic effect in superconductor.
- (II) In metallic elements, superconductivity is only found when the number of valence electrons per atom lies between two and eight.
- (III) In transition metal elements, the critical temperature varies in a periodic manner with the number of valence electrons per atom and exhibits sharp maximum. In non-transition elements, the critical temperature increases as the number of valence electrons per atom increases.

(IV) Low carrier concentration groups of superconductors are obtained by the addition of large amounts of appropriate impurities to semiconductors. Such as Ge, Tl etc.

The superconductivity, over these years has flourished as a field of scientific and technological endeavor, leading to the produce of many Nobel Laureates in physics. The Technological approach of superconductor is increasing rapidly, particularly in relation to computer switching element, bolometers, electromagnetic transportation, experimental science etc.

8.2 Historical Background

The history towards the direction of superconductivity starts from the liquefaction of helium by *Kamerlingh Onnes* in 1908. In 1911 *Onnes* discovered superconductivity in Hg at 4.2 K. In 1913, the superconductivity of lead at 72 K was discovered. It was observed in 1914 that superconductivity is destroyed by magnetic field. At critical magnetic field the superconductive state is destroyed. This discovery leads two conclusions of obstacle in the superconducting state i.e. temperature barrier and magnetic (or, corresponding critical current) barrier.

The magnetic or current barrier was overcome by the discovery of superconducting state in alloys in 1930s. Such types of superconductors are called type II superconductor. For such materials, superconducting state vanishes only above very high magnetic field of critical value $H_{c2}(T)$. Such as for Nb_3Sn , it is about 200 K Oersted. The endeavors to overcome the temperature continued until the investigation of metal oxide ceramics $BaPb_{1-x}Bi_xO_3$ (BPBO) in 1974. In this system for $x = 0.25$, the T_c was 13K. Until 1986, the T_c remained 24K only for Nb_3Ge a record. But after that *Bednorz* and *Muller* detected the appearance of superconductivity in the ceramic La-Ba-Cu-O(LBCO) with $T_c = 30-40K$. Table 8.1. gives some data on superconductors.

Later, towards the end of 1986, the existence of high temperature superconductor (HTSC), which can be called **Neon superconductors**, was reliably proved in Switzerland, Japan and USA for La-Ba-Cu-O and La-Sr-Cu-O (LSCO). In the beginning of 1987, La⁵⁷ was replaced by Y³⁹ and this led to the appearance of **Nitrogen Superconductor** with $T_c \approx 80-100K$. For example in $(Y_{0.6}Ba_{0.4})_2CuO_4$, the $T_c = 93K$ at atmospheric pressure. Similar result were obtained soon afterwards in USSR and able to get up to 102K using **Yttrium** of certain proportions. In 1993, H.R. Otto and his group in Germany broke the record of the high temperature superconductivity of that decade getting 133K in Hg-Ba-Ca-Cu-O. Next year in 1994 Chinese scientists observed 164K at 30GPA pressure in the same compound. However, no stable transition temperature greater than 138K at normal pressure is observed to date. It was recorded already in 1995 in the compound Hg-Tl-Ba-Ca-Cu-O. But now various scientists have obtained without a shadow of doubt, superconducting metal oxide ceramic of various compositions. Even for new Nitrogen superconductor, some non-reproducible results were obtained which could indicate the appearance of superconductivity with $T_c \approx 200-250K$. It can no means be ruled out that reliable information on the existence of room temperature superconductivity with $T_c \approx 250-300K$ will soon appear.

Theoretical study provides the causes of occurrence of superconducting state. There is really no good microscopic theory of superconductivity. What prevents from creating a new theory? Do scientists lack of additional facts or information or are waiting for the advent of a genius, a New *Einstein*?

To get theoretical knowledge of superconducting it had to wait until the discovery of super fluidity of He-II in 1938. It became then more or less clear that superconductivity is the super fluidity of electrons in metal. Then due to *Bose - Einstein* condensation and super fluidity, it is concluded that electrons in metals can be converted into bounded electron pairs with zero total spin. How electrons usually repel, can form a

Table 8.1 Properties of some selected superconductors in chronological order.

Year	T _c (K)	Material	Class	Crystal Structure	Type	H _c * (MAm ⁻¹)
1911	4.2	Hg	Metal	Tetragonal	I	0.033
1913	6.2	Pb	Metal	fcc	I	0.064
1930	9.25	Nb	Metal	bcc	II	0.164
1940	15	NbN	Interstitial	NaCl	II	12.2
1950	17	V ₃ Si	Compound	β -tungsten (W_3O)	II	12.4
1954	18	Nb ₃ Sn	Intermetallic Compound	W_3O	II	18.5
1960	10	Nb-Ti	Alloy	bcc	II	11.9
1964	0.7	SrTiO ₃	Ceramic	Perovskite	II	small
1970	20.7	Nb ₃ (Al, Ge)	Intermetallic Compound	W_3O	II	34.0
1977	23	Nb ₃ Ge	Intermetallic Compound	W_3O	II	29.6
1986	34	La _{1.85} Ba _{0.15} CuO ₄	Ceramic	Tetragonal	II	43
1987	90	YBa ₂ Cu ₃ O ₇	Ceramic	Orthorhombic	II	111
1988	108	Bi cuprates	Ceramic	Orthorhombic	II	—
1988	125	Tl cuprates	Ceramic	Orthorhombic	II	—
1993	133	HgBaCaCuO	Ceramic	Orthorhombic	II	—
1994	164	HgBaCaCuO at 30GPa	Ceramic	Orthorhombic	II	—
1995	138	HgTlBaCaCuO	Ceramic	Orthorhombic	II	—
2001	39	MgB ₂	Metallic		II	—

* extrapolated to 0K. H_{c2} for type II materials. (1 Oersted = 79.6 Am⁻¹)

bound state? In 1954, Ogy, reported that electrons are bound in pairs and *Bose-Einstein* condensation takes place by experimental way. Later *Ginsberg* and *Landau* gave a theory i.e. ψ -theory. *Schafroth* put forth the idea of pairing in most clear way and unmitigated suggesting that even the electron-phonon interaction could be responsible for pairing, but left unanswered about the nature and mechanism of pairing.

In 1956 *Cooper* introduced first pairing of electron called *Cooper pair*. Then the next year in 1957, the microscopic theory called reliable theory was first constructed, only 46 years after the discovery of superconductivity. It is known as *Bardeen, Cooper and Schrieffer* (BCS) theory. This theory concludes the following important results:

- The critical temperature of superconductor is *Debye* temperature (θ_D) dependant i.e.
$$T_c = 1.14 \theta_D e^{-\frac{1}{\lambda}} \lambda \text{ is coupling constant.}$$
- The energy gap in superconductor at transition temperature is $E_g = 3.52 K_B T_c$
- The specific heat capacity at transition temperature is $C_e = 1.43 \gamma T_c$ when γ is the coefficient of electronic specific heat
- T_c depends on mass and observed as $T_c \propto M^{-\frac{1}{2}}$ called isotopes effect.

8.3 Electric and Thermodynamic Properties

The different empirical electrical and thermodynamic properties of superconductor will be presented.

DC Resistivity

The first change to be discovered in superconductivity was the vanishing of electrical resistance as mentioned in earlier section. At the critical temperature, the DC resistivity vanishes and below it remains zero as shown in Fig. 8.1. The careful investigations have shown that the resistivity of a metal in the superconducting state drops to less than one part in 10^{17} of its value in normal state.

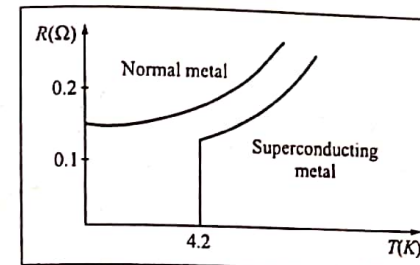


Fig. 8.1 Temperature dependence of the resistance of a normal metal and superconducting metal like Hg

AC Resistance

The zero resistance of the superconducting state is true only for DC of constant value. If the current is changing then a non zero resistance exists. For AC of a certain frequency, the resistance is both frequency as well as temperature dependent. It is also found that at high frequency the resistances in superconducting and normal states are equal. It is because, superconducting electrons are in a lower energy state than normal electrons, but if the frequency of the applied field is high enough, the photons of electromagnetic field have enough energy to exit superconducting electrons into the higher state where they behave as normal electrons. Such behavior is observed only above 10^{11} Hz.

Specific heat capacity

The specific heat capacity of a normal metal is in the form

$$C(T) = \gamma T + \beta T^3 \quad (8.1)$$

When first term represents the specific heat of electron in metal and the second is the contribution of lattice vibrations at low temperature. In superconducting state only electronic part is effected. So on subtracting the lattice contribution we will get as the form

$$C_{el}(T) = B e^{-\frac{\phi}{k_B T}} \quad (8.2)$$

Which shows the experimental variation of the electronic specific heat capacity with temperature and existence of a finite gap (ϕ) in the energy spectrum of electron separating two states.

At critical temperature, the specific heat capacity of the material increases abruptly. Fig 8.2 shows the variation of electronic specific heat with temperature.

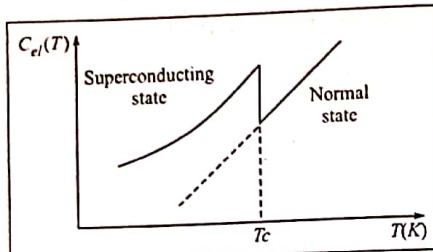


Fig. 8.2 Variation of electronic heat capacity with temperature

Thermal conductivity

The thermal conductivity of superconductor changes continuously between normal state and superconducting state as shown in Fig. 8.3. The value of thermal conductivity in superconducting state is lower than that in normal state which suggests that the electronic contribution drops in the superconducting state possibly playing no part in heat transfer. The thermal conductivity of tin at $2K$ is $34 \text{ wcm}^{-1} K^{-1}$ for its normal state and $16 \text{ wcm}^{-1} K^{-1}$ for its super conducting phase.

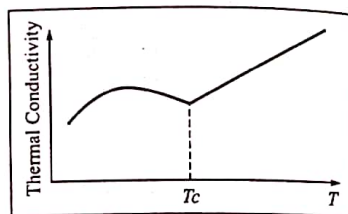


Fig. 8.3 Variation of thermal conductivity with temperature

The Energy Gap

It is well known that the exponential form is compatible with the thermal excitation across a gap in energy. This fact concludes an energy gap in the superconducting electron levels because of experimental nature of specific heat capacity in superconducting state of materials. Fundamentally, this gap differs from the energy gap in semiconductors or insulators. In superconductor the gap is related to Fermi gas and in semiconductor, the gap is attached to the lattice. The gap presents the flow of current in semiconductor whereas in superconductor current flows despite the presence of gap. From optical and many other methods, it is concluded that the gap energy is

$$E_g = 2\phi = 2b K_B T_c \quad (8.3)$$

$2b$ is constant and is about 3.5 for all materials. For gallium

$$E_g \approx 10^{-4} \text{ eV}$$

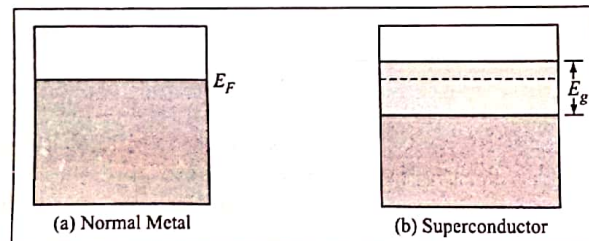


Fig. 8.4 Occupied and unoccupied states in (a) normal metal and (b) superconductor

8.4 Magnetic Properties

The magnetic properties of superconductors are unusual and unexpected. But magnetic properties are fundamental to superconducting state. The different magnetic properties are reviewed below.

The Meissner Effect

If a superconductor is cooled in a magnetic field from above the transition temperature then at the transition temperature and below, the lines of induction of B are pushed out.

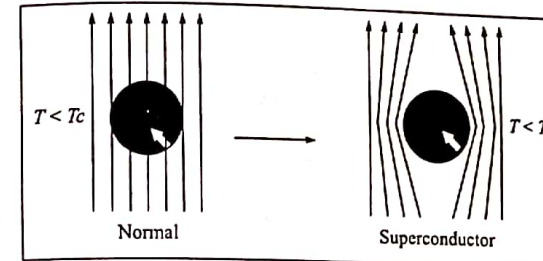


Fig. 8.5 Perfect diamagnetic effect in a superconducting state

This phenomenon was first discovered by Meissner and Ochsenfeld in 1933, and is called Meissner effect. It shows that a bulk superconductor behaves in an applied external field as if inside the specimen $B = 0$, i.e. perfect diamagnetic effect. Inside the superconductor $B = 0$. Thus

$$B = \mu_0 (H + M) = 0$$

$$\text{i.e. } H = -M \text{ and } \chi = \frac{M}{H} = -1$$

which is true for a perfect diamagnet.

The perfect diamagnetic behaviour of superconductor cannot be explained simply by considering zero resistivity. Now let an electric field E would accelerate superconducting electrons then

$$\begin{aligned} m \left(\frac{dv}{dt} \right) &= eE \text{ and super current density} \\ J_s &= n_s e v \\ \left(\frac{\partial J_s}{\partial t} \right) &= \left(\frac{n_s e^2}{m} \right) E \end{aligned} \quad (8.4)$$

i.e. if there is zero resistance, relaxational time would accelerate infinitely, which is not possible. So E must be zero inside the metal. From Maxwell's equation,

$$\nabla \times E = - \frac{\partial B}{\partial t} = 0$$

$$\text{i.e. } B = \text{Constant} \quad (8.5)$$

Thus B is constant in perfect conductor, which is contradiction to the *Meissner effect*. The behaviour of superconductor is different from that of a perfect conductor. Hence the superconducting state has mutually independent properties i.e. zero resistivity and perfect diamagnetism i.e.

$$E = 0 \text{ and } B = 0 \quad (8.6)$$

Materials showing such behaviour are known as soft or type I superconductors.

Critical Magnetic Field

A sufficiently strong magnetic field will destroy superconductor. The threshold or critical value of the applied magnetic field for the distribution of superconductivity is represented by $H_c(T)$ and is a function of temperature. At critical temperature the critical field is zero i.e. $H_c(T) = 0$

The Fig. 8.6 depicts the variation of critical magnetic field with temperature where S is superconducting state and N is normal state. The nature of the curve is approximately parabolic and satisfies the parabolic relation

$$H_c(T) = H_c(0) \left[1 - \left(\frac{T}{T_c} \right)^2 \right] \quad (8.7)$$

where $H_c(0)$ is the critical field at $0K$. Thus we find that the superconducting state is stable only in some definite ranges of magnetic fields and temperatures. For higher fields and temperatures, normal state is more stable.

Critical Current

In addition to $H_c(T)$ and T_c , a third critical parameter is often specified to a conductor. A given superconductor cannot support an electric current density greater than a critical value J_c which is temperature dependent and reaches a maximum at $T = 0K$. The critical current density and critical magnetic field are closely related because on passing current necessarily produces a magnetic field.

If a wire of radius a of type I superconductor carries a current I , a surface magnetic field H_I is set up. In addition if a transverse magnetic field H_a is applied to the wire, then the condition for transition to normal state is

$$H_c = H_I + 2H_a$$

i.e.

$$H_I = H_c - 2H_a$$

where $H_I = \frac{1}{2\pi a}$ and at critical value $I = I_c$

$$\therefore \frac{I_c}{2\pi a} = H_c - 2H_a$$

i.e.

$$I_c = 2\pi a(H_c - 2H_a) \quad (8.8)$$

Hence the critical current decreases linearly with increase of the applied field until $I_c = 0$ at $H_a = \frac{H_c}{2}$

This is also called *Silsbee's rule*. Fig 8.7 shows the variation of critical current density in a wire as a function of transverse applied field for pure and impure materials.

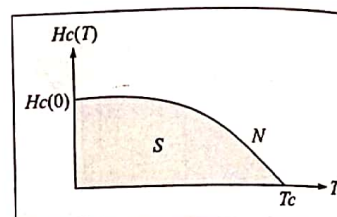


Fig. 8.6 Variation of critical field with temperature

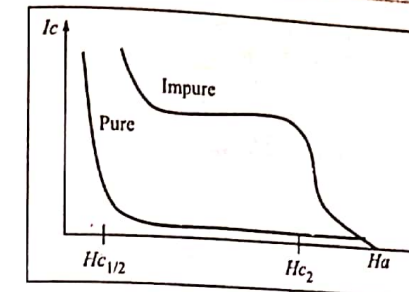


Fig. 8.7 Variation of critical current of pure and impure materials with transverse applied field

The London Equation

Two brothers F. and H. London in 1935 explained *Meissner effect* with two fluid models based on super fluid helium.

Electrical condition in normal state of a metal is described by *Ohm's law* which is to be modified to describe condition and *Meissner effect* in superconducting state. When a transitory electric field used to induce current in a sample, only the superconducting electrons flow while the normal electrons remained stationary and can be ignored as in equation (8.4)

$$\text{i.e. } \frac{dJ_s}{dt} = \left(\frac{n_s e^2}{m} \right) E$$

where n_s is the density of superconducting electrons.

Taking curl of both sides of this equation we get,

$$\frac{d}{dt} (\nabla \times J_s) = \left(\frac{n_s e^2}{m} \right) \nabla \times E$$

using *Maxwell's equation* $\nabla \times E = - \frac{\partial B}{\partial t}$ we get

$$\frac{\partial}{\partial t} \left[\nabla \times J_s + \left(\frac{n_s e^2}{m} \right) B \right] = 0$$

This equation cannot explain *Meissner effect* unless restricting and requiring the expression in square bracket be zero not just time dependence. So

$$\nabla \times J_s = - \left(\frac{n_s e^2}{m} \right) B \quad (8.9)$$

Again we have from *Maxwell's equation*

$$\nabla \times B = J_s$$

Again taking the curl on both sides of the relation we get

$$-\nabla^2 B = \nabla \times J_s$$

Hence from (8.9) we get

$$\nabla^2 B = \left(\frac{n_e e^2}{m} \right) B \quad (8.10)$$

This is called *London* equation of superconducting state of material where $\left(\frac{m}{n_e e^2} \right)^{\frac{1}{2}}$ is called *London* penetration depth and is represented by λ_L . The *London* equation is second order differential equation in B where ∇^2 is *Laplace* operator. Now the equation is

$$\nabla^2 B = \frac{B}{\lambda_L^2}$$

This equation occurs for the *Meissner* effect because it does not allow a solution uniform in space i.e. uniform magnetic field cannot exist in a superconductor. In pure superconducting state, the only field allowed is exponentially decayed as we go in from an external surface. Let a semi-infinite superconductor occupies the space on the positive side of x -axis, then the solution of the *London* equation for this case will be

$$B(x) = B(0) e^{-\frac{x}{\lambda_L}} \quad (8.11)$$

where $B(0)$ is the field at the plane boundary. The penetration depth λ_L measures the depth of penetration in which field decreases by a factor e^{-1} . If thickness of the specimen is very less than λ_L , *Meissner* effect is incomplete and it $\lambda_L \ll x$, field damps out exponentially inside the superconductor. So λ_L is the fundamental length that characterises a superconductor.

Coherence Length

The superconducting is due to mutual interaction and correlation of the behaviour of electrons which extend over a considerable distance. The maximum distance up to which the states of pair electrons (cooper pairs) are correlated to produce superconducting state is called coherence length. Hence coherence length is the measure of the minimum spatial extent of a transition layer between normal and superconductor. Any spatial variation in the state of an electronic system requires extra kinetic energy. A modulation of an

eigen function increases the kinetic energy because of the increase of integral of $\frac{d\phi}{dx^2}$.

Let the kinetic energy of a plane wave, $\psi = e^{ikx}$ is given by

$$E = \int \psi \left(-\frac{\hbar^2}{2m} \nabla^2 \right) \psi^* dx = -\frac{\hbar^2}{2m} \int \psi^* \left(\frac{\partial^2 \psi}{\partial x^2} \right) dx$$

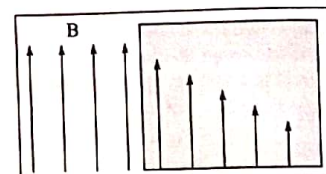


Fig. 8.8 Penetration of an applied magnetic field into a semi-infinite superconductor.

$$E = \frac{\hbar^2 k^2}{2m}$$

i.e.

where $\psi \psi^* = 1$ but for the strongly modulated wave function

$$\phi(x) = \frac{1}{\sqrt{2}} (e^{i(k+q)x} + e^{ikx}) \text{ the corresponding kinetic energy is}$$

$$E = \int \phi^* \left(-\frac{\hbar^2}{2m} \nabla^2 \right) \phi dx$$

$$= -\frac{\hbar^2}{2m} \int \phi^* \frac{\partial^2 \phi}{\partial x^2} dx$$

$$= \frac{1}{2} \left(\frac{\hbar^2}{2m} \right) [(k+q)^2 + k^2]$$

$$E = \frac{\hbar^2}{2m} k^2 + \frac{\hbar^2}{2m} qk \quad (8.13)$$

where $q \ll k$. Thus the increase of energy required to modulate the wave is $\frac{\hbar^2 k q}{2m}$. If this increase exceeds the energy gap E_g , superconducting state will be destroyed. The critical value of q is q_0 of the modulation wave vector for normal $k = k_F$ is then

$$E_g = \frac{\hbar^2}{2m} k_F q_0 \quad (8.14)$$

Now we can define the intrinsic coherence length ξ_0 as

$$\xi_0 = \frac{1}{q_0} = \frac{\hbar^2 k_F}{2m E_g} = \frac{\hbar V_F}{2E_g} \quad (8.15)$$

where V_F is electron velocity in *Fermi* surface. Hence coherence length is a measure of the distance within which the gap parameter (E_g) cannot change drastically in a spatially varying magnetic field.

8.5 Type I and Type II Superconductor

The superconductor in which the *Meissner* effect is complete up to critical field H_c is called type I superconductor. The magnetic behaviour of a typical type I superconducting is shown in Fig. 8.9. These material give away their superconductivity at lower field strength so these are referred to as soft superconductors. Pure specimens of various metals exhibits this type of behaviour.

Surface energy of a material is a result of magnetic field which is positive for type I superconductor. Another important feature of the type I superconductor is exhibiting an intermediate state between superconducting state and normal state. However a cylinder placed in parallel magnetic field does not exhibit intermediate state. The coherence length of type I superconductor is greater than penetration

depth. Such as for Sn, $\xi_0 = 23 \times 10^{-6}$ cm and $\lambda_L = 3.4 \times 10^{-6}$ cm, and for Al $\xi_0 = 160 \times 10^{-6}$ cm and $\lambda_L = 1.6 \times 10^{-6}$ cm. The mean free path of type I superconductor is greater than penetration depth. Pure lead having $\xi_0 = 8.3 \times 10^{-6}$ cm and $\lambda_L = 3.7 \times 10^{-6}$ is a type I superconductor exhibiting the magnetizing curve I in Fig. 8.10.

But when some amount of indium is doped to the lead, the behaviour will no longer type I. It shows the curve II type behaviour, which is characteristics of type II superconductor. These types of materials tend to be alloys, ceramic or hard transition metals with high value of electrical resistivity at normal state i.e. low value of mean free path in normal state. In such type of materials, superconducting state exists up to H_{c2} . Between the lower critical field H_{c1} and upper critical field H_{c2} , $B \neq 0$ i.e. Meissner effect is incomplete. The region between H_{c1} and H_{c2} is called Vortex State. The critical field of He is 4.8×10^4 A/m at 4K and when 20% indium is added it becomes type II superconducting of which $H_{c1} = 3.6 \times 10^3$ A/m and $H_{c2} = 2.9 \times 10^5$ A/m. Surface energy of type II superconductor is negative so vortex state or mixed state is stable. It is also observed that the penetration depth (λ_L) of these superconductors is larger than coherence length (ξ_0). These superconductors are also called hard or impure superconductor.

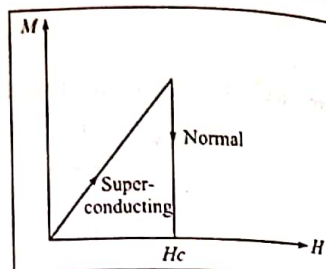


Fig. 8.9 Magnetization curve of Type I superconductor. The graph plots Magnetization (M) on the vertical axis against Magnetic Field (H) on the horizontal axis. A straight line starts from the origin (0,0) and extends upwards to a point labeled 'Normal'. At a certain magnetic field H_c , the line meets a horizontal line labeled 'Super-conducting'. The region between the two lines is shaded.

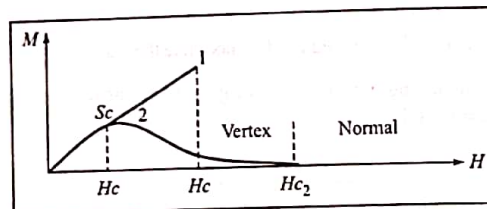


Fig. 8.10 Magnetization Curve

8.6 The BCS Theory

In 1957 almost half a century after the discovery of superconductivity, a comprehensive microscopic theory of superconducting phenomenon was proposed by Bardeen, Cooper and Schrieffer called BCS theory. This theory helps to overcome the difficulties to pair that the electrons are fermions and repulsive force among them take away from each other. The main BCS theory is described using the basic three phenomena:

Electron-phonon interaction

According to Frohlich, when an electron moves through a crystal it produce lattice distortion and sets the heavier ions into slow vibrations. Since the electron moves very fast leaving this region much before the oscillation can die off. This slightly increases the density of the positive ion cores in the intermediate region of the electron and polarizes the crystal. Other electrons in this region with high density of positive ions are attracted. Hence the electrons are attracted to each other via the movement of ions.

The interactions between (I) electron-electron and (II) electron-phonon or lattice will be strong enough to overcome the coulomb force. The net effect is the attraction of two electrons via a lattice distortion to

form a pair of electrons known as cooper pair. This can also be expressed by Isotope effect. The large electron-phonon interaction would be expected to lead to high temperature superconductor and also leads high resistance in normal state.

Cooper pair

As described above the lattice vibration plays an important role and due to interaction if wave vector (k_1) of an electron is equal and opposite to another ($-k_2$), results an attractive force with same energy, which causes the electrons to exit in pair. It is also shown that the interaction is larger for the electrons with opposite spins because they have larger probability of being close to each other. The coherence length is used to measure the size of cooper pair. If $B_E = 2Eg$ be the binding energy of the pairs, i.e. cooper pairs then

$$\xi_0 = \frac{\hbar V_F}{B_E}$$

i.e. the size of pair depends on Fermi velocity and binding energy. It is of the order of 10^{-4} cm. All electrons in the metal tend to form such pairs k with $-k$ and that this electron gas undergoes a Bose - Einstein condensation.

BCS Ground State

In non-interacting Fermi gas, all state below Fermi surface are occupied and above it are vacant. The lowest excited state is separated from ground state by an arbitrary low excitation energy. But the phonon assisted attractive interaction between electrons gives rise to the BCS ground state. This is separated from the lowest excited state by a finite energy gap Eg . The BCS state appears to have a higher kinetic energy than the Fermi state, but the attractive potential energy of BCS state decreases, i.e. the BCS state is more stable than Fermi state.

The BCS ground state differs from ground state of non-interacting Fermi gas.

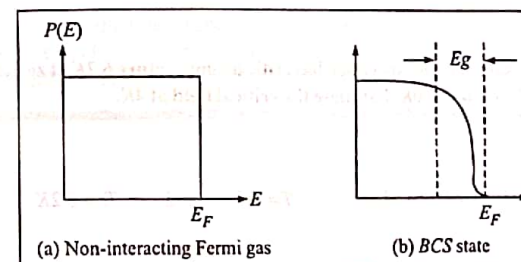


Fig. 8.11 Probability of occupancy versus energy of (a) non-interacting Fermi gas and (b) the BCS ground state

The superconducting state is a condensed in the source that a finite energy Eg is required to produce an excited state of the whole system. It is a bit like a semiconductor, but in semiconductor energy gap is tied to the Brillouin zone and the superconductor energy gap is carried by Fermi surface.

8.7 Material Aspects

First superconducting state was observed in Hg by Kamerlingh Onnes in 1911. The T_c of Hg was 4.2K. Later 1973 J.R. Gavaler observed 22.3K in Nb_3Ge . A new class of oxide ceramic superconductor having the

196 Electrical Engineering Materials

critical temperature greater than 30K was discovered by Bednorz and Muller in 1986 which developed a new era in the field of superconductivity. These are called high T_c - superconductors. The first group of such materials are $\text{La}_{2-x} \text{M}_x \text{CuO}_4$ ($\text{M} = \text{Ba}, \text{Sr}, \text{Ca}$) with T_c ranging from 35K to 40K and is referred to as 214 system. Another system of the material is $\text{M Ba}_2 \text{Cu}_3 \text{O}_{7-y}$ with $y = 0.2$ and ($\text{M} = \text{Te}, \text{Y}, \text{Nd}, \text{Sm}$ etc) is called 123 system. Other system are Bi-Sr-Ca-Cu-O (BSCCO) with onset temperature of 110K and Tl-Ba-Ca-Cu-O (TBCCO) of 118K are also found.

The BSCCO and TBCCO contain planes of Cu- and O- atoms. But in YBCO compound have both planes and chains of Cu- and -O- atoms. Planes plays the major role in generating superconductivity while chains acts as electron reservoirs which can be filled or emptied either by changing the O-Stoichiometry or doping. These compounds have orthorhombic structure with distortion and almost always exhibit twinning. It was speculated that the twin planes in YBCO samples are a source of high temperature superconductivity. But this idea became less convincing after the development of Tl and Bi compound which do not have twin plane.

Properties of high T_c superconductor:

1. High T_c which is an appreciable function of Debye temperature (θ_D) and is given by $T_c \approx \theta_D e^{-\frac{1}{\lambda}}$ where λ is coupling constant characterizing the intensity of attraction.
2. Short coherence length: which is temperature dependence and is the consequence of the BCS theory $\xi = \xi_0 \left(1 - \frac{T}{T_c}\right)^{-\frac{1}{2}}$
3. Large anisotropy: Tl based superconductors are most anisotropic than any other superconductors. Such as Bi, La or Y based compounds.

8.8 Examples

1. The superconducting state of a lead specimen has critical temperature 6.2K at zero magnetic field and the critical field is 0.064 MAm^{-1} at 0K. Estimate the critical field at 4K.

Solution:

We have

$$H_c(0) = 0.064 \text{ MAm}^{-1}, \quad T = 4K \quad \text{and} \quad T_c = 6.2K$$

Also we have,

$$H_c = H_c(0) \left[1 - \left(\frac{T}{T_c} \right)^2 \right]$$

$$= 0.064 \left[1 - \left(\frac{4}{6.2} \right)^2 \right] = 0.037 \text{ MAm}^{-1}.$$

Hence the critical field of Pb at 4K is 0.037 MAm^{-1} .

2. Calculate the size of a cooper pair if the gap energy is 10^{-3} eV and Fermi velocity of the electron is 10^6 ms^{-1} .

We have,

$$h = 1.055 \times 10^{-34} \text{ Js} \quad V_F = 10^6 \text{ ms}^{-1} \quad BE = 10^{-3} \text{ eV} = 10^{-3} \times 1.6 \times 10^{-19} \text{ J}$$

Then using relation

$$\xi_0 = \frac{hV_F}{BE} = \frac{1.055 \times 10^{-34} \times 10^6}{1.6 \times 10^{-22}} = 4 \times 10^{-7} \text{ m}$$

Thus the size of cooper pair is $4 \times 10^{-7} \text{ m}$ and is comparatively longer than the distance between two electrons ($\approx 10^{-10} \text{ m}$)

Exercise

1. Determine the temperature at which the critical field becomes half of its value at 0K if the critical temperature of a superconductor at zero magnetic field is T_c . [0.707 T_c]
2. The BCS theory of superconductivity shows that the superconducting energy gap at 0K is $3.5k_B T_c$. Calculate the maximum wavelength of microwave radiation that will be absorbed at 0K in lead. [0.57 mm]
3. Determine the critical current which can flow through a long thin superconducting wire of aluminium of diameter 1mm. The critical magnetic field for aluminium is $8 \times 10^3 \text{ Am}^{-1}$. [24.80 A]
4. Calculate the coherence length of an aluminium if the size of the energy gap is $3.4 \times 10^{-4} \text{ eV}$ and Fermi velocity is $2.02 \times 10^6 \text{ ms}^{-1}$. [3.9 $\times 10^{-6} \text{ m}$]
5. For a superconducting specimen, the critical field are 1.4×10^5 and $4.2 \times 10^5 \text{ Am}^{-1}$ for 14K and 13K. Estimate the transition temperature and critical fields at 0K and 4.2K. [14.5K, 20.7 $\times 10^5 \text{ Am}^{-1}$ and $18.9 \times 10^5 \text{ Am}^{-1}$]
6. A niobium superconducting solenoid carries current 20A to produce $6 \times 10^4 \text{ Am}^{-1}$. Estimate the minimum diameter of wire that may be used in the solenoid if it is immersed into liquid helium at 4.2K. The critical field for niobium is $1.56 \times 10^5 \text{ Am}^{-1}$. [1.16 mm]